Vibration Based Blind Identification of Bearing Failures in Rotating Machinery

Rohit Gopalkrishna Sorte[1], Pardeshi Ram[2]

Department of Mechanical Engineering, Mewar University, Gangrar, Rajasthan

Abstract: ***Present paper deals with a suitable tests rig, which can help in determination the vibration in wind mill or other rotating machinery with the help of Test rig assembly, which can be further utilized to check on the behaviour of bearing in various corrupted noise and signal. Therefore we can know the early fault in bearing to avoid loss of cost production and catastrophic accident. So it is important to detect incipient faults. In condition monitoring, the early detection of incipient bearing signal is often made difficult due to its unusual noise by background vibration. Hence it is essential to minimize the noise of component in the observed signal. This paper shows that the proposed technical with optimum filter length does improved the signal and can be used for automatic feature extraction and fault classification. This technique has potential for use in wind mill or rotating machine diagnostics.***

Keywords: Signal-Noise-Ratio (SNR), Corrupting signal, Noise, Filter, Frequency.

1. Introduction

A bearing in a machine element that constrains motion and reduces friction between moving parts to only the desired motion. Therefore bearing is main unit of any types of machines. Bearing failure is one of the foremost causes of failure in rotating machinery. The bearing guiding the shaft should have good thermal properties strength and load bearing capacity. The friction between shafts should be low in order to get good power transmission. Condition monitoring for early detection of faults to prevent catastrophic failure in running industries. Vibration measurement are used for detection of defects in bearings [1].

This paper focused on the development of reliable method for detection of vibration or fault occur in rotating machine
1. Recognize type of damage of bearing
2. Offer possible cause for bearing damage
3. Suggestion for the prevention of damage

Limits of catastrophic Failure

Should bearing occur, determination of the root cause of failure required evidence to remain in the bearing. I order to accomplish this, preventive maintance technic can be used to catch bearing failures before they become catastrophic.

Noise

Noise is audible sound heard by equipment technicians. It is important to distinguish normal sounds from the pump system is not operating clearance excessive clearance, damage contact area, contamination and unsuitable lubricant.

Vibration

Many common problems in machines such as imbalance, play, misalignment can best be evaluated by measuring vibration displacement or velocity. Vibration is measured using accelerometers mounted on the equipment. There are standards for evaluation machine performance based on vibration.

Table 1: Evaluation of Vibration velocity [cm/s] rms

Evaluation	Vibrational velocity[cm/s] rms	
	Rigid supports	Flexible supports
Good	Less than 0.18	Less than 0.28
Satisfactory	0.18~0.46	0.28~0.71
Unsatisfactory	0.46~1.12	0.71~1.8
Unacceptable	More than 1.12	More than 1.8

Cause of vibration in bearing
Excessive load
Overheating
True brinelling
False brinelling
Normal fatigue failure
Reverse loading
Contamination
Lubricant failure
Corrosion
Misaligned bearings
Loose fits
Tight fits and etc,.

Instrument for Data Acquisition

The whole experiment set up to collect fault signal. The experiment consist of fault bearing, accelerometer, a charge amplifier, an external filter, Labview interface and data acquisition software.

Experimental Test Rig

This experimental Test Rig capable of simulating common machine fault, gear damage, shaft misalignment a defective roller element like bearing and other fault. As shown in symmetric diagram Figure 1

A damage bearing is set up on position3 and fault measuring signal from position 2and 3 with different speed. The ability to drive the damage and undamaged bearing signal to be observed simulation. Were vibration response of bearing with defect and no defect where measured with different speed.

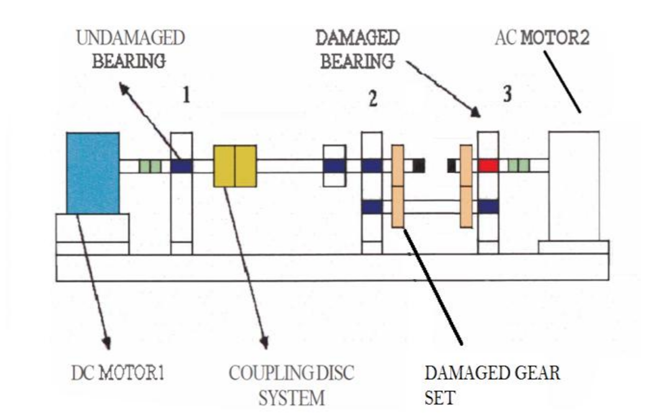

Figure 1: Schematic of test rig.

Accelerometer

A piezoelectric sensor is a device that used the piezoelectric effect, to measure charge in pressure, acceleration, vibration, strain or force by converting then to a electric charge. These devices utilize mass in direct contact with the piezoelectric component when a varying motion is applied to the accelerometer, the crystal experiences a varying force excitation (F=ma), causing a proportional electric charge q to be develop across it [2].

So where q is the charge developed and **dij** is the piezoelectric coefficient of the material. As this equation shows, the output from the piezoelectric material is dependent on it mechanical properties, **dij**

q=dijF=dij ma.................................. (1)

Charge Amplifier

In order to transform the high output impedance of the accelerometer into a lower value and to amplify the relatively weak output signal from the accelerometer into a lower value and to amplify the relatively weak output signal from the accelerometer, a pre-amplified is required for data acquisition. The charge amplified is used to get rid of variable accelerometer cable length. The only necessary information is the charge sensitivity of accelerometer.

Data Acquisition

A NI connector, model NI BNC2120 and NI DAQ6062E data acquisition card were used to convert an analog signal to the digital. Labview was used to record and analyse data convert the analog data into a digital sequence for off-line analysis.

Benchmark Blind Deconvolution Tests

Bearing failure is one of the foremost causes of breakdown in rotating machinery. Whenever a defect on rolling element of bearing of a bearing interacts with mating element, abrupt changes in the element generates a pulse or impact of very short duration due to vibration and resulting noise which can be monitored

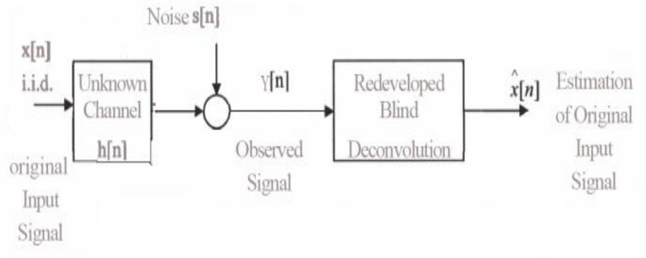

Figure 2: Redeveloped Blind Deconvolution Diagram

Bearing fault signal x[n] which is transmitted through unknown channel h[n] contamination noise s[n], observed signal y[n]. the redeveloped Blind Deconvolution algorithm is used to recover the original source signal x^[n] estimation of original input signal.

Simulation of Blind Fault Signal

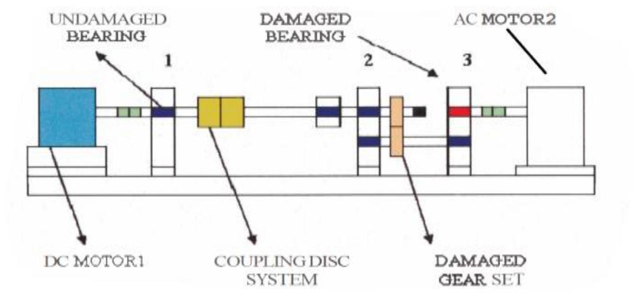

Figure 3: Schematic of test rig.

The test bearing consist of deep groom bearing 6201 was damaged using 0.1 mm cut to a outer race was placed in position3. The DaqEZ professional data acquisition software package was used to collect and analyses. Ball pass frequency (BPFO) can be calculated

$$BPFO = {}^{n}/_{2}\left(1 - \frac{B_d}{P_d}\cos 8\right)s \ldots\ldots\ldots\ldots\ldots\ldots\ldots\ldots \quad (2)$$

Where, n=number of roller element, B_d= $\left({}^{\O d_a - \O d_a}/_{2}\right)$ (D_a&d_a=outer & inner race diameter) P_d= pitch diameter, 8= angle of contact, s =revolution per second.

Measuring signal from position 2and 3 is damaged bearing and signal are collected from different position 2and 3. All the signals contain information of the faults and can be used for fault detection. Collecting signals from damaged bearing signal from position 3 and 2, damage bearing signal from position 3 and 2 plus noise of damage gear [3].

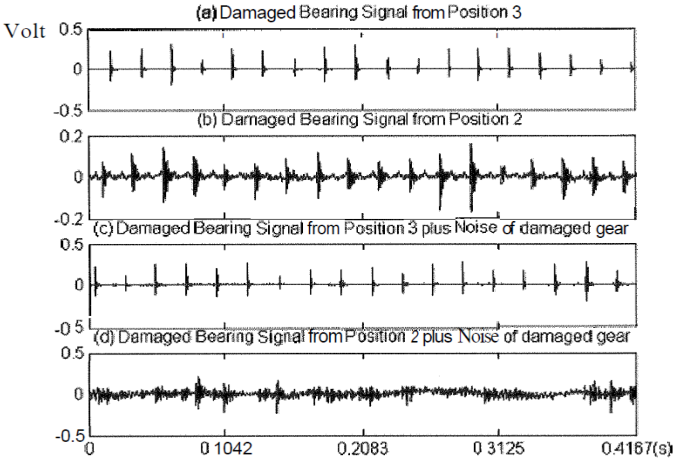

Figure 4: Measured signal from different positions

Periodic Noise

The technique of blind deconvolution is as based on its ability to recover the input signal when the channel is unknown. The robustness of blind deconvolution can be tested by corruption the observed signal with simulated noise.

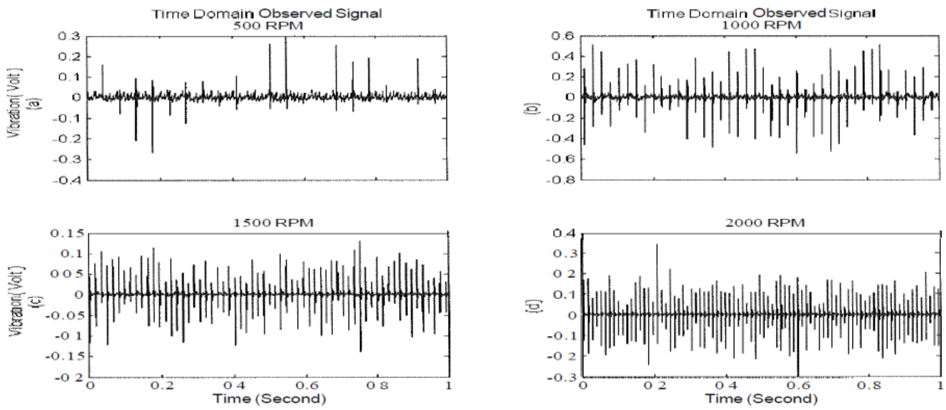

Figure 5 Defective bearing signals recorded at different speed (a) 500RPM; (b) 1000 RPM; (c) 1500 RPM; (d) 2000RPM.

These simulated noise can be divided into two categories; deterministic the amplitude and frequency of the generated noise was weird to produce different signal to noise–ratio (SNR). These different SNR are-8dB to-43.9dB.

Figure **6(a)** Rotating speed 500RPM corrupted by 500Hz sinusoidal noise with -8dB SNR which can shown in figure 6(b). Figure **6(c)** show that blind deconvolution technique removed sinusoidal noise with a -8dB SNR. The filter length of equalize was selected by trail and error.

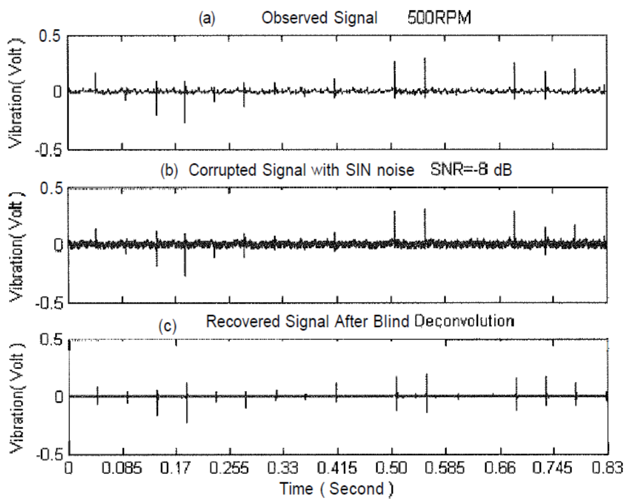

Figure 6: (a) Observed signal with 500RPM (b) Corrupted signal with sinusoidal noise with 500Hz and SNR=-8dB (c) Recovered signal using blind deconvolution

In figure 7(a) rotating speed 500RPM corrupted by 500Hz sinusoids noise with -20dB SNR which is shown in figure 7(b). Figure 7(c) shown that the blind deconvolution technic removed sinusoidal noise with a -20dB SNR and recovering a clear signal a close as possible to the source signal.

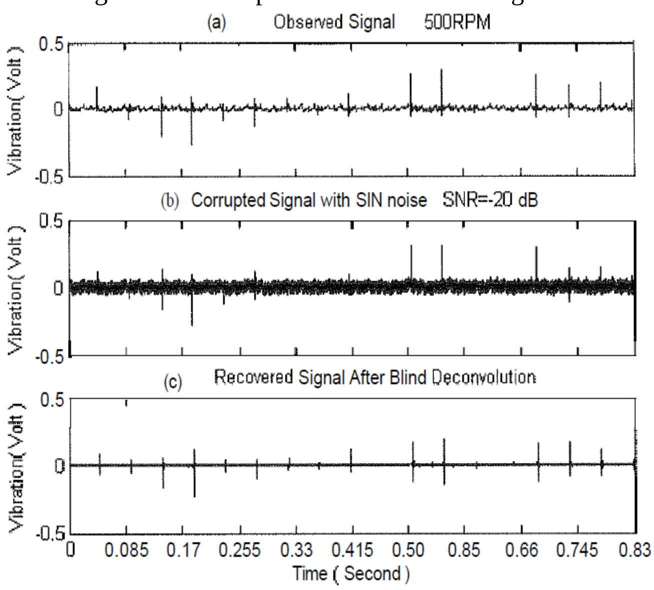

Figure 7: (a) observed signal with 500RPM (b) Corrupted signal with sinusoidal noise with 500Hz and SNR=-20 dB (c) Recovered signal using blind deconvolution.

In figure 8(a) rotating speed 500RPM corrupted by 500Hz sinusoids noise with -43.93dB SNR which is shown in figure

8(b). Figure 8(c) shown that the blind deconvolution technic removed sinusoidal noise with a -49.93dB SNR and recovering a clear signal a close as possible to the source signal.

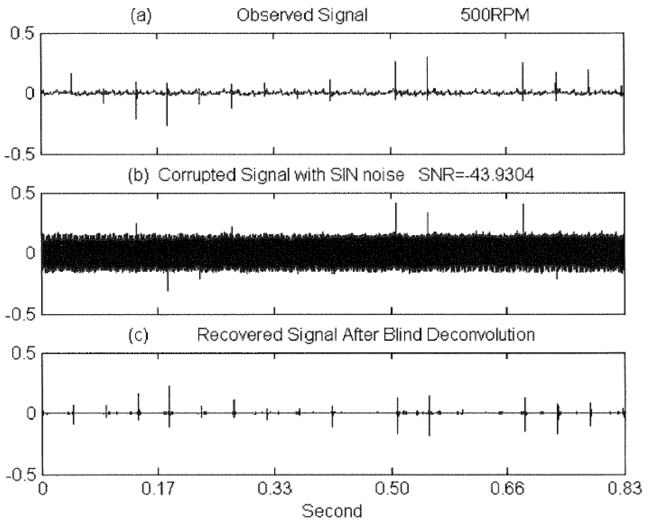

Figure 8: (a) observed signal with 500RPM (b) corrupted signal with sinusoidal noise with 500Hz and SNR=-43.9304dB (c) Recovered signal using blind Deconvolution.

Time Interval Averaging

In order to minimise the error calculating the mean (Bias) and the variance of estimated time interval between the impacts it is required to collect signal [3, 4, 6, 7]. The time period (interval between impacts) of the recovered signal after blind deconvolution was calculated using pre-set threshold to get rid of minor fluctuation , as well as unknown noise which come from other components[8]. Then next large peak is found and W sample around peak are set at zero. The value of W taken less than half of interval samples. The detected time interval between impacts can be regarded as random variable since the outcome of each experiment can be different. Table 2 shown the result of ten different observation in terms of four speeds.

Table 2: Average Frequency (Time Interval) of all Time Intervals

Shaft Speed (Observation)	500 RPM	1000 RPM	1500 RPM	2000 RPM
1st	20.35 Hz	41.77 Hz	62.56 Hz	83.93 Hz
2nd	21.82	42.32	62.41	83.71
3rd	22.86	42.39	62.52	83.68
4th	23.50	41.17	61.61	83.89
5th	21.82	43.71	62.89	83.67
6th	24.16	42.36	62.82	83.73
7th	19.80	41.84	63.15	83.71
8th	21.62	40.58	60.28	84.40
9th	22.88	42.37	62.85	83.63
10th	24.11	43.53	62.39	83.71
Average (Hz)	22.27	42.20	62.37	83.81
BPFO	**21.21**	**42.42**	**63.63**	**84.84**

Taking average of all interval for each speed, time between impacts and compared with BPFO in Equation 3. It can be seen in table 2. Average Frequency (Time interval). The variation is there frequency valves at each speed is due to the constant speed was not maintained during data collection.

The performance of blind deconvolution can be evaluated more effectively if the original input sigh of channel is already known. Using sum of the squared deviation (SSD) of each sample estimated signal $x^a[n]$ and original input signal x[n] [9].

$$SSD = \sum_{i=1}^{N} \lfloor x^{A}[n] - x[n] \rfloor^{2} \quad \text{.................................} \quad (3)$$

There are some other criteria used instead of SSD such as full width at the half maximum(FWHM) [10].this criteria is independent of input signal and useful when the width of the impact signal measured in time domain when wave is considerable high recovering signal x[n] with observed signal y[n] by employing a trimmed standard deviation(TSD).

$$TSD = \left[\frac{1}{N-2T} \sum_{i=T-1}^{N-T} (X^{\wedge}_{i} - TM)^{2}\right]^{1/2} \quad \text{.........................} \quad (4)$$

Where N the number of samples of the recovered sorted signal $X^{\wedge}_{i}$ and;

($X^{\wedge}_{i}$ 1 2, …N), where $X_1 \le X_2 \ldots\ldots\ldots \le X_N$

The value of TSD is an indication of noise in the signal and is a measurement of energy. The trimmed mean, TM, is defined as:

$$TM = \frac{1}{N-2T} \sum_{i=T-1}^{N-T} X^{\wedge}_{i} \quad \text{....................................} \quad (5)$$

Where, T is the length of truncated samples with the nearest integer y~ where y is the percent of the highest and lowest data. Small values of TSD indicate a good estimation of the inverse filter. In this experiment the filter length was set at 32 and the number of block samples at L=N=12000. The value of TSD was computed with fixed y =0.05 to exclude the largest and the smallest spikes. The calculated TSD for the observed and recovered signals are shown in Table 3 TSD of the observed and recovered signals. The results show that the values of TSD for the recovered signals are reduced when compared to the values of TSD for the observed signals for each speed. This is because the impulsive bearing fault signals are extracted by blind deconvolution and the contaminating noise is suppressed. Hence a reduced TSD value for the recovered signal is obtained [11].

Table 3: TSD of the observation and recovered signals

Shaft Speed	Observed Signal y[n]	Recovered Signal x^[n]
500RPM	0.034	0.008
1000RPM	0.053	0.017
1500RPM	0.067	0.021
2000RPM	0.067	0.028

Summation of Periodic Noise

The most fundamental cause of noise are called varying compliance vibration it is irrespective manufacture quality and accuracy of bearing.

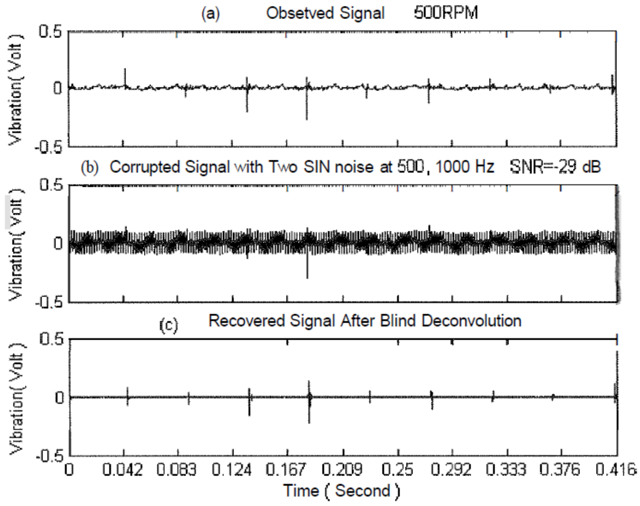

Figure 9: (a) Observed signal at 50Hz (b) Corrupted signal with combination of 2 sinusoidal noise at 500, 1000 Hz (c) Recovered signal after blind Deconvolution.

The bearing fault signal with a rotational speed of 500RPM shown in figure 9(a), was corrupted with periodic noise 500 and 1000Hz random filter length was applied to corrupted signal to obtain recovering signal figure 9(b) shows than capability of removing noise with a -29dB SNR and recovering a clean signal.

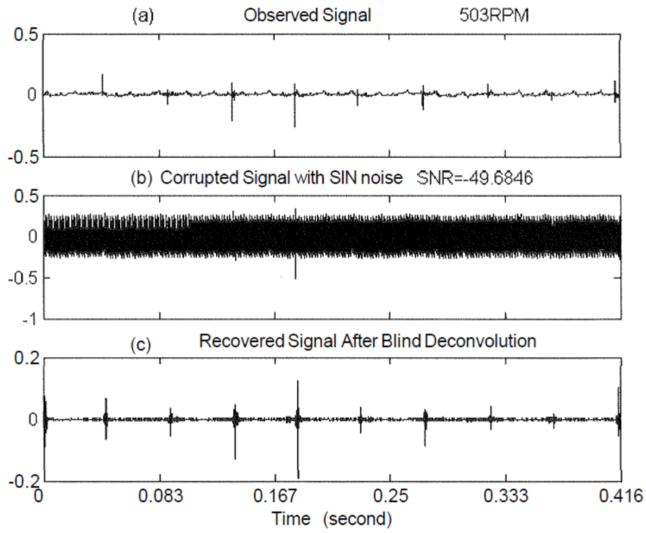

Figure 10: (a) observed signal at 500Hz (b) corrupted signal with summation of 5 sinusoidal noise frequencies at 25, 500, 1000, 2000 and 4000 Hz (c) Recovered signal after BD.

The bearing fault signal was further modified using a summation of five different periodic noise frequency in figure 10(b) i.e. 25, 500, 1000, 2000Hz original vibration signal is corrupted by simulated noise and the bearing fault impact are invisible figure 10(c) shown that capability of removing sinusoidal noise with a very low -49.64dB SNR and recovering a clear signal as close as possible to the source signal.

3.3 Determining Blind Deconvolution Effectiveness and Optimum Filter Length

3.3.1 Plan for Bearing Damage

In order to optimize filter length based on the general conditions of a vibration signal including type of fault on the bearing components, nine Koyo 6201 ball bearings were damaged according to the specifications presented in Table 3.3 Defect specifications of bearings.

Table 1.4: Defect specifications of bearings

Number	Fault location and type		
	Outer Race (width)	Inner Race (width)	Ball (diameter)
	Crack		Spot
1	0.1	0.1	0.1
2	0.2	0.2	0.2
Quantity	2	2	2

Table 3.4 Different speeds of experiments, indicates three different speeds, cut off frequency and sampling frequency for each experiment. Sets of data with different operational conditions were collected to provide data training sets as discussed in the theory of determining filter length in Chapter 3. Table 3.5 Data files for the simulation experiments, presents data files for the simulation experiments. In Table 3.5, C is the configuration number and A is the amplifying factor.

Table 5: Different speeds of experiment.

RUN No.	Speed	Cut off Frequency	Sampling Frequency
1	600RPM	10kHz	40kHz
2	1200RPM	10kHz	40kHz
3	1800RPM	10kHz	40kHz

Table 6: Data files for the simulation experiments

Size (mm)	Speed (RPM)	Healthy			Ball			Inner race			Outer race		
		Name	C*	A*	Name	C*	A*	Name	C*	A*	Name	C*	A*
0.1	600	H1	1	0.1	BS1	1	0.1	IS1	2	10	OS1	1	0.1
	1200	H2	1	0.1	BS2	1	0.1	IS2	2	10	OS2	1	0.1
	1800	H3	1	0.1	BS3	1	0.1	IS3	2	1	OS3	1	0.1
0.2	600				BM1	1	0.1	IM1	2	10	OM1	1	0.1
	1200				BM2	1	0.1	IM2	2	10	OM2	1	0.1
	1800				BM3	1	0.1	IM3	2	1	OM3	1	0.1

Measured Bearing Damage Signals

Outer Race Defect Experiments

In Figure 11 the size of fault is 0.1 mm in width. In Figure 11 three different speeds are plotted 500, 1200 and 1800 RPM

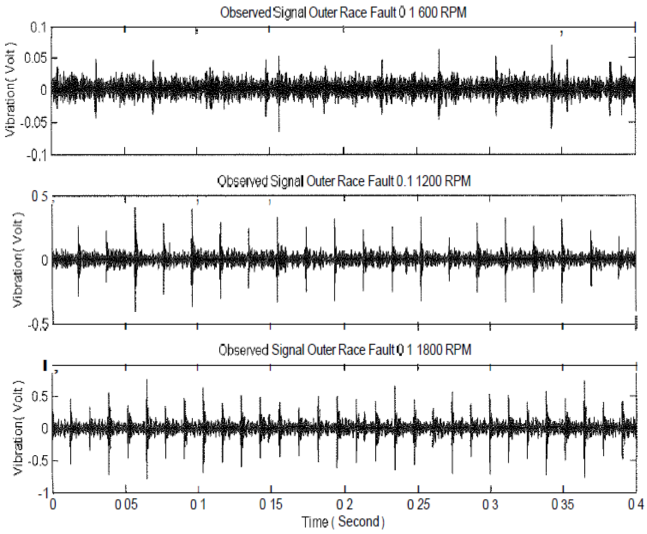

Figure 11: A typical observed signal for an outer race fault 0.1mm rotating at (a) 600 RPM (b) 1200 RPM (c) 1800 RPM.

Figure 12 In Figure 11 the size of fault is 0.2 mm in width. In Figure 12 three different speeds are plotted 500, 1200 and 1800 RPM

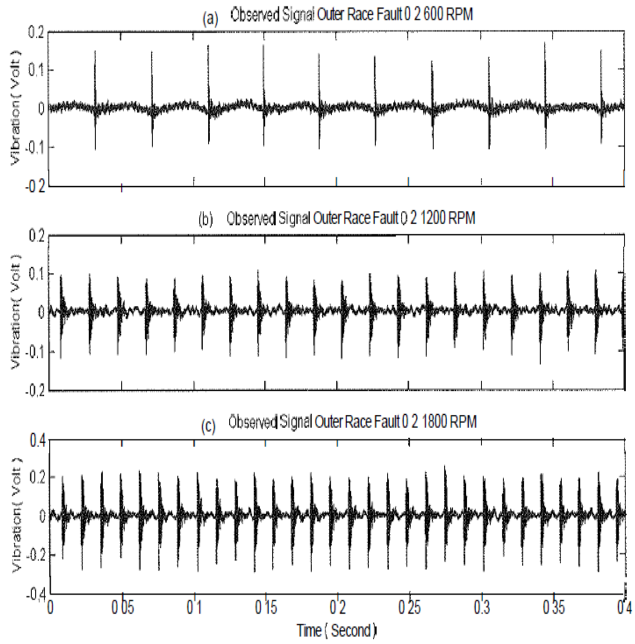

Figure 12: A typical observed signal for an outer race fault 0.2mm rotating at (a)600 RPM (c)1200 RPM (c) 1800 RPM

The characteristic defect frequency is computed for each speed, matched with the average time interval between the impacts.

Inner Race Defect Experiments

In figure 13 the size of fault is 0.1 mm in width. In Figure 13 three different speeds are plotted 500, 1200 and 1800 RPM

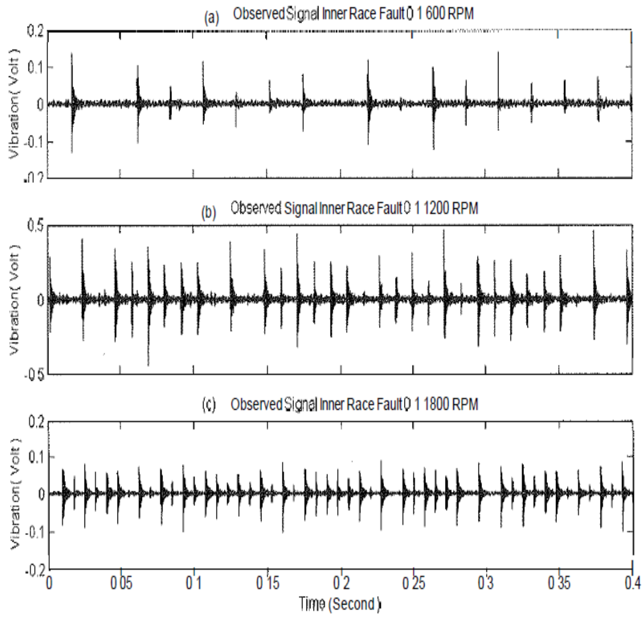

Figure 13: A typical observed signal for an inner race fault 0.1mm rotating at (a) 600 RPM (b) 1200 RPM (c) 1800 RPM.

In Figure 14 the size of fault is 0.2 mm in width. In Figure 3.28 three different speeds are plotted 500, 1200 and 1800 RPM

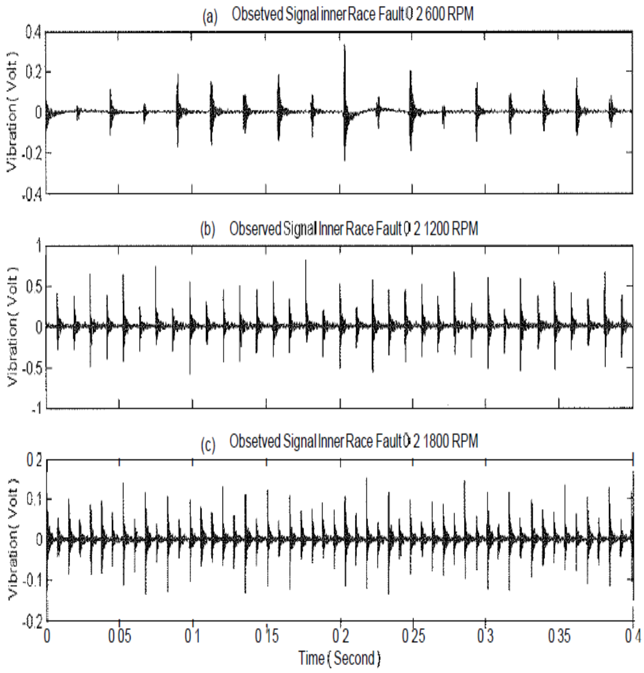

Figure 14: A typical observed signal for an inner race fault 0.2mm rotating at (a) 600 RPM (b) 1200 RPM (c) 1800 RPM

The characteristic defect frequency is computed for each speed, matched with the average time interval between the impacts.

3.3.3.3 Ball Race Defect Experiments

Figure 15 represents a typical observed signal from a ball defect experiment. The fault of 0.1mm in width and with three different speed at 500, 1200 and 1800 RPM.

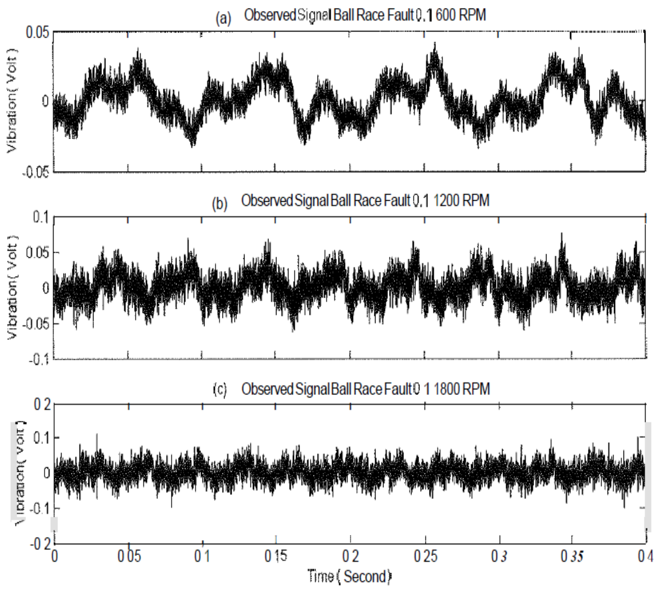

Figure 15: A typical observed signal for a ball fault with 0.1 mm in diameter rotating at (a)600 RPM (b) 1200 RPM (c) 1800 RPM

Figure 16 represents a typical observed signal from a ball defect experiment. The fault is 0.2mm in width and with three different speed at 500, 1200 and 1800 RPM.

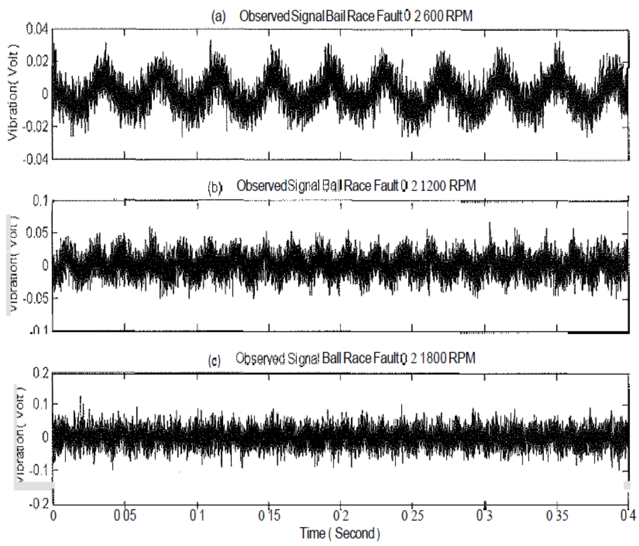

Figure 16: A typical observed signal for a ball fault with 0.2 mm in diameter rotating at
(a) 600 RPM (b) 1200RPM (c) 1800RPM

The characteristic defect frequency is computed for each speed, matched with the average time interval between the impacts in all three defects 0.1 and 0.2 mm.

Faults Detection using optimum Filter Length

Fault position with 600RPM and 0.1 mm outer race defect in figure 17(a) and frequency spectrum in figure17(b) the modified crest factor (CF) and Arithmetic Mean (AM) of recovered signal plotted with varying filter length from 2 to 240 FIR in figure 17(c) and 17(d). Figure 17(c) indication that the average peak gets large over the RMS value. In figure 17(d) AM amplitudes fluctuated between -75dB to -90dB until 186 filter length amplitude constant about -98dB. Because CF value increases AM value decreases and both treads remain constant.

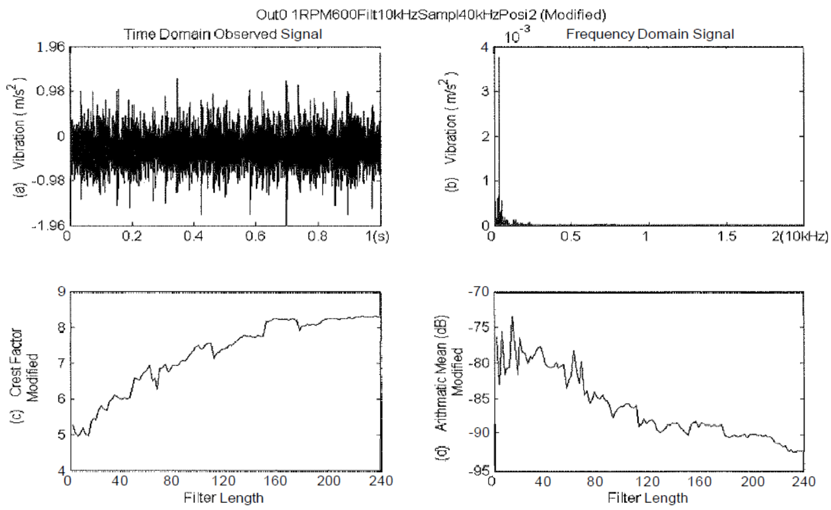

Figure 17: (a) Observed signal of an outer race defect at 600RPM
(b) Observed signal in frequency (c) Modified crest factor graph versus length of the equalizer (d) Arithmetic mean graph versus filter length

The top trace of Figure 18 illustrates the observed signal with an outer race defect rotating at 600 RPM and the bottom trace shows the recovered signal with the optimum filter length. In the left top trace, it is not possible to see the damaged bearing signal and the impulses are masked by background noise. The bottom trace shows a consistent

International Journal of Science and Research (IJSR)
ISSN (Online): 2319-7064
Index Copernicus Value (2013): 6.14 | Impact Factor (2013): 4.438

impulsive signal of a damaged bearing with an average time interval of 0.039 seconds very close to the characteristic defect frequency. A healthy bearing with Gaussian distribution has a kurtosis value close to 3. The kurtosis of the observed signal was found to be 2.78 because it indicates a Gaussian distribution, while the kurtosis of the recovered signal was 9.06 and it can be seen that the recovered signal was improved. Figure 19 shows the result of a demodulation process performed on the recovered signal with the outer race defect shown in Figure 17. In the demodulation process, the signal was filtered with band pass between 5000 and 7500 Hz which was to be the correct bands pass to be the range that would result in the detection of the best characteristic frequency (25.5 Hz). The reason for this is that the characteristic defect frequency with a dominant spike at 25.6 Hz is clearly visible in the spectrum which is close to the calculated frequency of 25.5 Hz. The spike is accompanied by a number of harmonics spaced at multiples of the characteristic frequency.

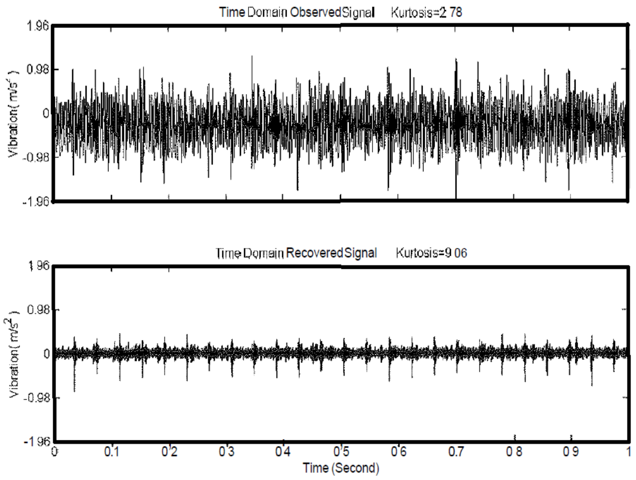

Figure 18: Top-Observe signal with an outer race defect, kurtosis=2.78, bottom-recovered signal with the optimum filter length L=186, kurtosis=9.06

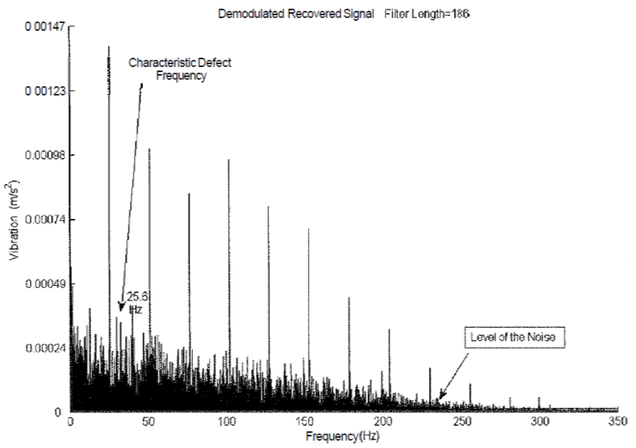

Figure 19: Demodulated recovered signal at 600 RPM with outer race defect

3.3.6 Removing the High Resonance Frequency Components

As a result of optimum filter length, an observed signal with an outer race defect of 0.1 mm width RPM was input to the blind deconvolution algorithm. The results are presented in Figure 3.42(a). It can be observed from Figure 3.42(b) that the observed signal of an outer race defect of 0.1 mm and rotating speed of 600 RPM was further corrupted with 500 Hz sinusoid noise to mask the impacts. It can be seen from Figure 3.42(c) that blind deconvolution has recovered the source of vibration sufficiently to identify the impacts. It can be seen that blind Deconvolution with optimum filter length has enhanced the original bearing signal and has eliminated the background noise. The impulses from the defect on the outer race can be clearly seen and the SNR has been improved.

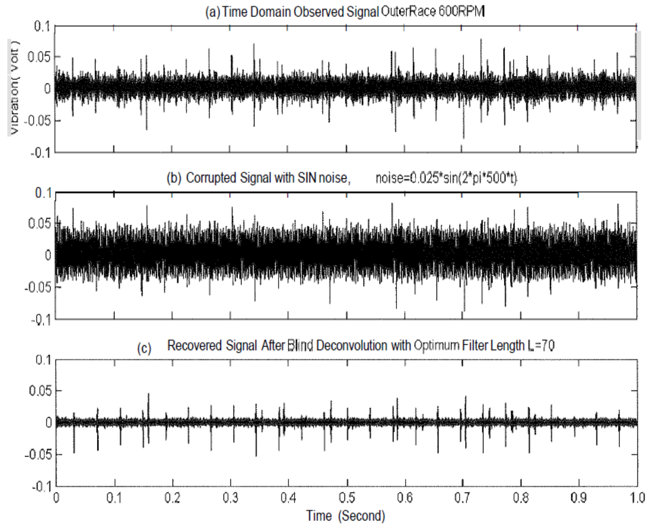

Figure 3.42: (a) Observed signal at 600RPM (b) Corrupted signal with sinusoid noise (c) Recovered signal after the blind Deconvolution algorithm

2. Conclusion

In this paper, we presented a methodology for reliability calculation under different speed, vibration signal, corrupted signal noise and etc. Monitoring noise, vibration, temperature and lubrication can help to find out problems before bearing failure. Vibration measured in time domain and frequency domain are key points for doing work. So, we will use time domain and frequency domain for extraction of fault and diagnosis in one work. Although the phenomenological description exhibits similarities for those cases, the effects on the system are particularly different. Still, the identification of natural frequency excited by the impact is a valuable of the impact loading on general system.

References

[1] Janko Slavic, AleksandarBrkovic, Mihaboltez, “Typical Bearing-Fault Rating Using Force Measurement-Application to Real Data”, Journal of Vibration and Control, December 2011 vol.17 no 14 2164-2174
[2] E. D. I. Division, "Shock and vibration measurement technology," 1976, pp. 10-7, 10-8
[3] D. Dyer and R. Stewart, M.., "Detection of rolling element bearing damaged by statistical vibration analysis," Trans ASME, JMech Design, vol. 100, pp. 229-235, 1978.
[4] A. F. Stronach, C. J. Cudworth, and A. B. Johnston, "Condition monitoring of rolling element bearings," Proceedings of the International Condition Monitoring

Conference, *Swansea*, UK, 10-13, pp. 162-177, 1984.

[5] R. Prabhu, "Rolling bearing diagnostics," Proceedings of the Indo-US Symposium on Emerging Trends in Vibration and Noise Engineering, New Delhi,, pp. 311-320, 1996.

[6] P. Y. Kim, "A review of rolling element bearing health monitoring : preliminary test results on current technologies," Proceedings o Machinery Vibration Monitoring and Analysis Meeting, Vibration Institute, New Orleans, LA, 26-28, pp. 127-137, June 1984.

[7] D. Dyer, "Bearing condition monitoring," Interim Report 1 Department of Mechanical Engineering, University of Southampton, Southampton (UK), 1973.

[8] J.-Y. Lee, Nandi, A.K.,, "Blind deconvolution of impacting signal," Seismic Engineering- ASME, vol. 387, 1999.

[9] A. I .Nandi, D. Mampel, and B. Roscher, "Blind deconvolution of ultrasonic signals in non -destructive testing," IEEE Trans. on Sig. Proc., vol. 45(5), pp. 1382-1393, 1997.

[10] J.-Y. Lee, Nandi, A.K.,, "Blind deconvolution of impacting signal using higher-order statistics," Mechanical Systems and Signal Processing, vol. 12(2), pp. 357-351, 1998.

[11] J.-Y. Lee and A. K. Nandi, "Extraction of impacting signals using blind deconvolution," Journal of Sound and Vibration, vol. 232, pp. 945-962, 2000.

Author Profile

Rohit Gopalkrishna received the B. Tech degree in Mechanical Engineering from Mewar University, Rajasthan. At present perusing the Master of Technology in Manufacturing System Engineering at Mewar University, Chittorgarh, Rajasthan.

Pardeshi Ram received his M. Tech degree in Production Engineering from Indian Instituted Technology, Banaras Hindu University. Pardeshi Ram is an Assistant Professor, Department of Mechanical Engineering in Mewar University, Chittorgarh, Rajasthan.